

# HELIOSEISMIC CONSTRAINTS ON ROTATION AND MAGNETIC FIELDS IN THE SOLAR CORE

PHILIP R. GOODE

*Big Bear Solar Observatory, New Jersey Institute of Technology, 40386 North Shore Lane, Big Bear City, CA 92314, U.S.A.*

(Received 31 May 2000; accepted 6 November 2000)

**Abstract.** In recent years, more and more precise measurements have been made of solar oscillation frequencies and line widths. From space, the *Solar and Heliospheric Observatory*/Michelson Doppler Imager (MDI) data has led to much progress. From the ground, networks, like Global Oscillation Network Group (GONG), Taiwanese Oscillation Network (TON), and Birmingham Solar Oscillations Network (BiSON) have also led to much progress. The sharpened and enriched oscillation spectrum of data have been critically complemented by advances in the treatments of the opacities and the equation of state. All of this has led to a significantly more precise probing of the solar core. Here we discuss the progress made and suggest how the core may be better probed with seismic data on-hand. In particular, we review our knowledge of the rotation and structure of the core. We further argue that much may be learned about the core by exploiting the line width data from the aforementioned sources. Line-width data can be used to place sharper constraints on core properties, like the degree to which the Sun rotates on a single axis and the upper limit on magnetic fields that may be buried in the core.

## 1. Introduction

The Sun's vitality arises in its nuclear burning core. Understanding this region is of broad interest. However, probing the solar core is a difficult matter. Our best chance is exploiting  $p$ -mode data. The problem is that  $p$ -mode power is concentrated near the solar surface. This is indirectly illustrated in Figure 1, where we show the averaging kernels for structural inversion for the  $\ell = 0$  and  $\ell = 80$  modes with frequency closest to 3 mHz. There, we also indicate that the location of the innermost bump in the  $\ell = 0$  kernel is a fairly strong function of frequency. In particular, the  $\nu = 4.7$  mHz mode has a bump centered at  $0.06 R_{\odot}$ , while if  $\nu = 1.6$  mHz, the bump moves all the way out to  $0.16 R_{\odot}$ . Thus, to be successful, the inverter requires modes covering as wide a range of  $\ell$ -values as possible, with as broad a frequency range as possible. Clearly, the low- $\ell$  modes best probe the core. The equation in Figure 1 is the high-frequency limit of the oscillation equations. This simple equation tells us what the figure illustrates – the inner turning point is deeper for higher frequency and lower  $\ell$  modes.

The useable width of the spectrum in frequency is limited at both the high and low ends. Solar oscillations are driven very near the solar surface (Goode *et al.*, 1998b). As can be seen in the equation in Figure 1, the outer turning point of



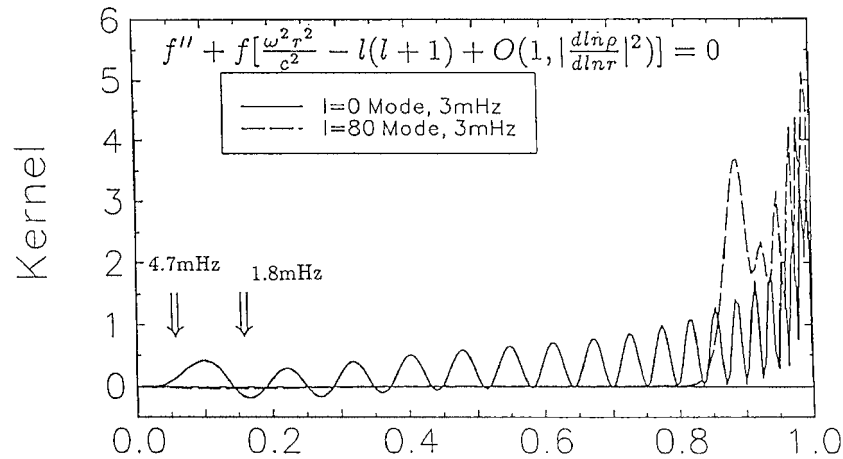


Figure 1. Averaging kernels for 3-mHz modes of  $\ell = 0$  and 80 are shown as a function of fractional radius. The location of the innermost bump for  $\ell = 0$  is shown for 1.8-mHz and 4.7-mHz modes, respectively. The oscillation equation is shown in the high-frequency limit from which it is clear that the inner turning point for a mode depends on both its frequency,  $\omega$ , and its  $\ell$ -value.

the modes is deepest (furthest from the surface) for the lowest frequency modes. Thus, these modes don't reach the excitation region very well, and are very weakly excited, and therefore have lower amplitudes. The highest frequency modes tend to leak from the cavity. Thus, they are not so seismically useful because they have overly broad line widths and ill-defined frequencies – both reflecting their short lifetimes.

For rotation, some of the lowest- $\ell$  kernels are illustrated in Figure 2 (Chaplin *et al.*, 1999). It is clear that the differential probing of the solar core rests on having as broad a frequency spectrum as possible for the oscillation data. These kernels illustrate the difficulty in determining the rotation rate in the innermost part of the solar core.

The problem of probing the solar core is further complicated by the fact that the mode frequencies evolve during the solar cycle. However, this problem is soluble.

## 2. Near-Surface Perturbation Due to Activity

Kuhn (1988) was the first to realize that the frequency of solar oscillations varies systematically through the solar cycle. Libbrecht and Woodard (1990) showed that the frequency changes are due to a near-surface perturbation associated with the activity cycle. Although the perturbation which changes the frequency lies very close to the surface, this does not preclude a deeper lying origin of the near-surface perturbation. To probe the nature of the perturbation, Dziembowski and Goode (1991) and Goldreich *et al.* (1991) developed formalisms to describe the near-surface perturbation. For our purposes here, we need to determine it, so that we

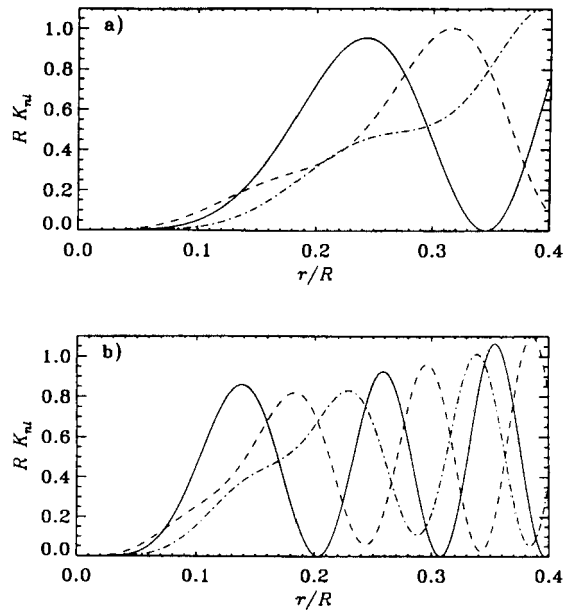


Figure 2. (a) Rotational kernels for modes near 1.5 mHz:  $\ell = 1, 2, 3$  – solid, dashed, dot-dash, respectively. (b) For modes near 3.0 mHz, from Chaplin *et al.* (1999).

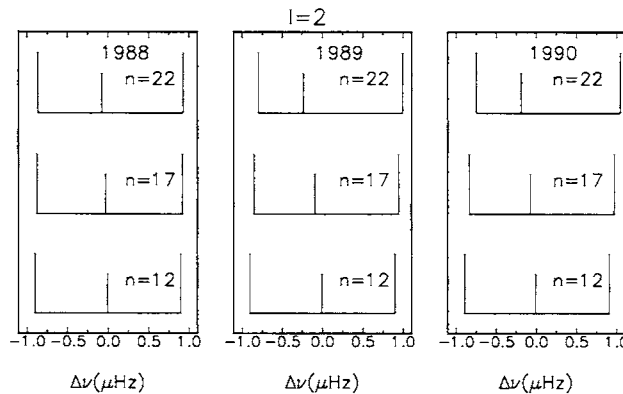


Figure 3. The  $(\ell + m)$ -even fine structure peaks, which are those which would be detected in whole-disk observations, are shown for  $\ell = 2$  and for  $n = 12, 17,$  and  $22$  as a function of frequency. From left to right are times of increasing solar activity, and the non-uniform spacing arises from the near-surface effect of activity, rather than any variation in the core.

can remove it from the data. The removal is critical for a proper interpretation of Sun-as-a-star data. One can use intermediate  $\ell$ -data to determine the near-surface perturbation, and then remove the effect of the perturbation from the Sun-as-a-star data. After removal, one then can use the residual data to probe the core.

For each  $p$ -mode multiplet, the individual mode frequencies,  $\nu_{\ell,n,m}$ , are represented by

$$v_{\ell,n,m} - \bar{v}_{\ell,n} = \sum_{k=1}^{\ell} a_k \mathcal{P}_k^{\ell}(m), \quad (1)$$

where  $\mathcal{P}$  are orthogonal polynomials (see Ritzwoller and Lively, 1991; and Schou, Christensen-Dalsgaard, and Thompson, 1994). This representation ensures that the  $\bar{v}_{\ell,n}$  are a probe of the spherical structure while the  $a_{2k}$  – the even- $a$  coefficients – are a probe of the symmetrical (about the equator) part of the distortion described by the corresponding  $P_{2k}(\cos \theta)$  Legendre polynomials. We have

$$C_{k\ell} \mathcal{P}_{2k}^{\ell}(m) = \int_0^{2\pi} \int_{-1}^1 |Y_{\ell}^m|^2 P_{2k} d(\cos \theta) d\phi, \quad (2)$$

where

$$C_{k\ell} = (-1)^k \frac{(2k-1)!!}{k!} \frac{(2\ell+1)!!}{(2\ell+2k+1)!!} \frac{(\ell-1)!}{(\ell-k)!}. \quad (3)$$

The splitting coefficients in Equation (1) are inverted using the following formula (Dziembowski and Goode, 1991):

$$a_{2k,\ell,n} = a_{2k,\ell,n;\text{rot}} + C_{k,\ell} \frac{\gamma_k}{I_{\ell,n}}, \quad (4)$$

where  $a_{2k,\ell,n;\text{rot}}$  represents the effect of centrifugal distortion, which we calculate following the treatment of Dziembowski and Goode (1992);  $I_{\ell,n}$  is a measure of the modal inertia (also called the mode mass), and  $\gamma_k$  is the asphericity coefficient corresponding to a  $P_{2k}$  distortion.

The  $\gamma$ s are strong functions of their Legendre rank, but are weak functions of frequency. They also vary systematically through the solar cycle. This variation can trick the unwary inverter, see Figure 3. To illustrate this, we follow Dziembowski and Goode (1996) who considered low- $\ell$  modes from whole disk observations. In this case, it is assumed that the Sun is rotating uniformly and the effect of the near-surface perturbation due to activity is included, as determined from intermediate- $\ell$  data from Big Bear Solar Observatory (BBSO), using Equation (4).

In Figure 3, it is quite clear that at times of high activity, the modes which most strongly sample the near-surface would have an observed spacing which is not uniform. Since these modes are also the ones that best sample the deep interior, one might naively argue for a solar cycle change in the core. However, it is clear that this is a surface effect. That is the bad news. The good news is the surface effect can be calculated using intermediate  $\ell$  data, and then removed from the low- $\ell$  data, allowing one use the residual to probe the core.

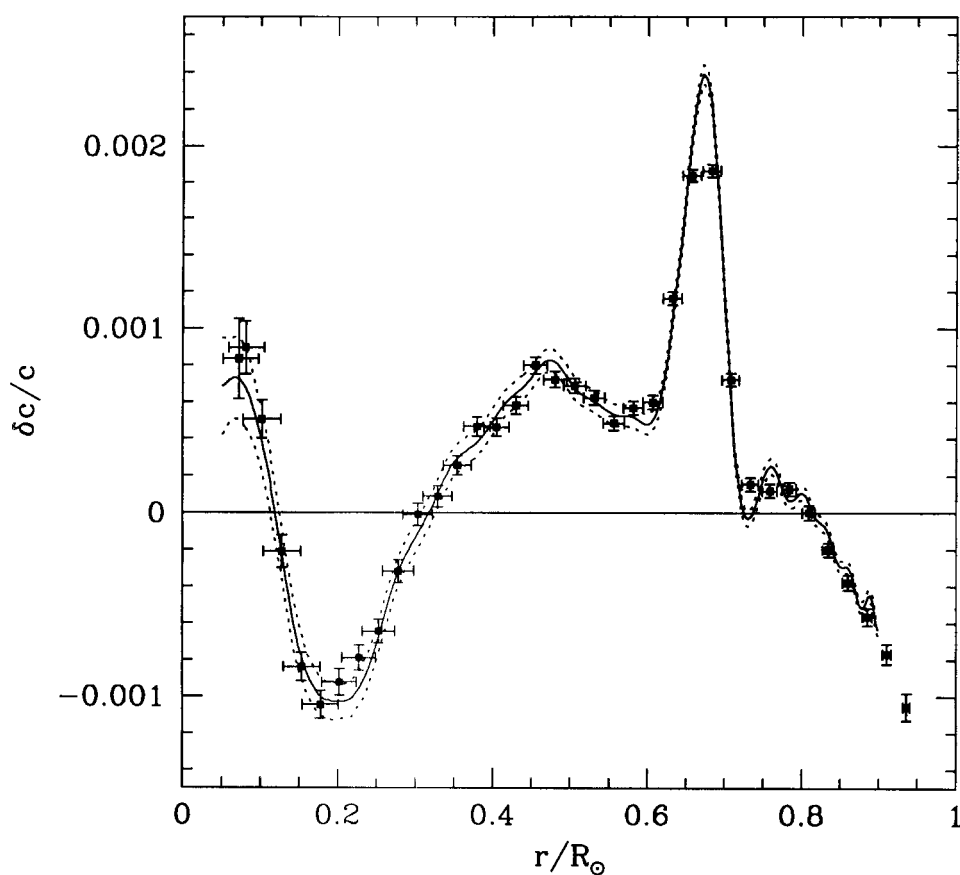


Figure 4. Structural inversion of the solar core showing the fractional difference between the model and seismic speed of sound vs. the fractional solar radius (Basu *et al.*, 2000) using MDI data.

### 3. Probing the Core

#### 3.1. THE STRUCTURE

The seismic probing of the solar core has become more and more precise over the last decade. This results from ever more precise and extensive oscillation data, and improved treatments of the opacities and equation of state. In Figure 4, one can see that with the exception of the region just beneath the base of the convection zone, we know the run of the speed of sound to better than one part in a thousand. This is more than fifty times more accurately than we knew this number a decade ago. This evolution has been driven by the oscillation data, and has led to significant advances in our understanding of stellar evolution theory.

The bump in Figure 4 lying just beneath the convection zone is the only place where the disagreement is more than one part in a thousand. The bump tells us that there is a convective overshooting for which the solar models have not accounted.

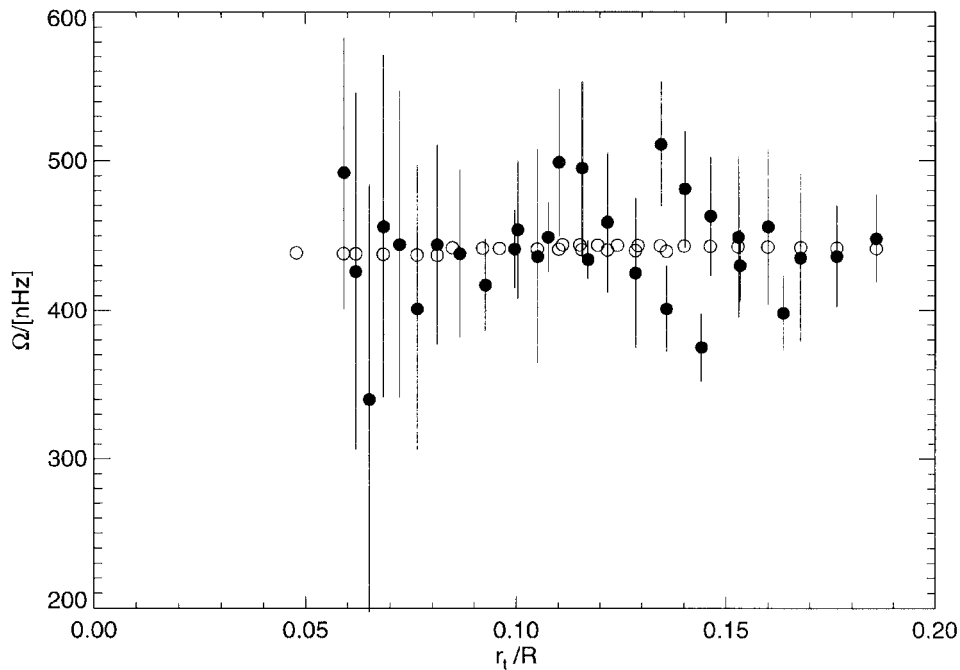


Figure 5. Rotational frequency vs. fractional radius. The *open circles* are the splittings assuming rigid rotation, and the *solid circles* are the splitting data (Bertello *et al.*, 2000).

It is this kind of interaction between observations and models which has advanced stellar evolution theory over the last decade.

### 3.2. ROTATION

The Sun's differential rotation is becoming more and more precisely known. Duvall, Harvey, and Pomerantz (1986) used their South Pole oscillation data to show that the Sun's convection zone exhibits surface-like differential rotation. Brown *et al.* (1989) and Dziembowski, Goode, and Libbrecht (1989) showed that there is a sharp transition toward solid-body rotation beneath the base of the convection zone. We know that the transition is rather sharp. For a recent discussion, see Chaplin *et al.* (1999).

As for the rotation in the core, the progress has been slower. But recently, Bertello *et al.* (2000) solved a forward problem, see Figure 5, demonstrating that it is reasonable to think that down to  $0.05 R_{\odot}$  that the rotation in the equatorial plane is that of a rigid body.

### 3.3. ASPHERICITIES IN THE CORE

It would be of great interest to discover asymmetries seated in the deep interior. Unfortunately, a preliminary analysis of the SOHO/MDI data does not give us

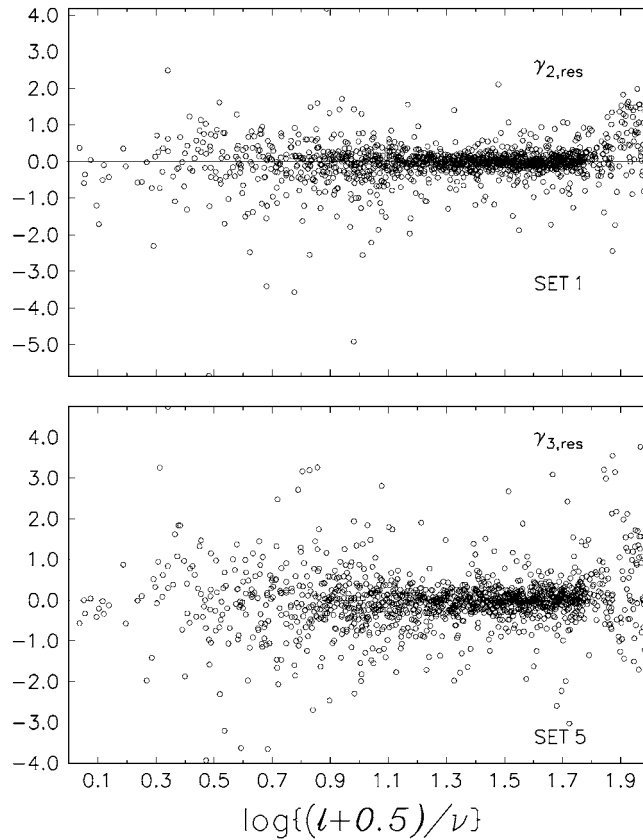


Figure 6. The residual  $\gamma_{k,\text{res}}$  (see Equations (3) and (4)) for  $k = 2$  and  $3$  for selected sets vs. the inner turning point of the mode associated with the residual. The *upper panel* is for the MDI set beginning 1 May 1996 and the *lower panel* is for data beginning 13 February 1997. Each set covers 72 days.

much reason for hope at this time (Goode *et al.*, 1998a). Although that may change with new, and longer strings of data. The residuals of the  $a_{2k,\ell,n,\text{res}}$ , after removing the centrifugal term and the  $\gamma$  term, do not exhibit a visible dependence on the position of the inner turning point. It is well known that  $p$  modes preferentially sample the region just above their inner turning points.

In Figure 6, we plot the quantities

$$\gamma_{k,\text{res}} = \frac{a_{2k,\ell,n,\text{res}} c_k}{I} \quad (6)$$

for  $k = 2$  and  $3$  for sets 1 and 5 of the MDI data. Recall that the MDI data come in 72-day long sets. Set 1 covers 72 days starting 1 May 1996, and set 5 starts 13 February 1997. Both sets cover times of relatively low solar activity. In Figure 6, the residuals are plotted against a parameter,  $\lambda$ , which determines the position of the lower turning point. We see no trend in the distribution of the residuals about the zero-line, except, perhaps for some preponderance of positive values above  $\lambda = 1.8$

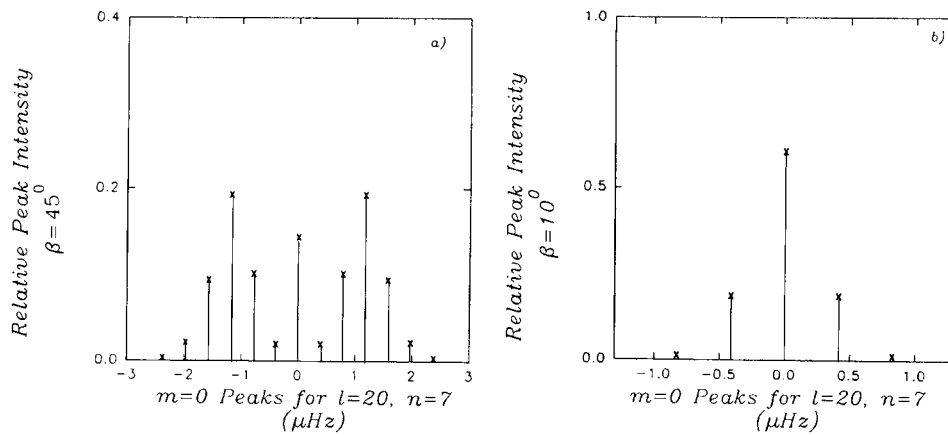


Figure 7. Relative intensity of  $m = 0$  peaks for the  $\ell = 20$  1894  $\mu\text{Hz}$  mode under the assumption the axis of rotation of the radiative interior is tipped, by an angle  $\beta$ , with respect to that of the convection zone. Only peaks with more than 0.1% of the total intensity are shown. *Left panel* has  $\beta = 45^\circ$  and *right panel* has  $\beta = 10^\circ$ .

which corresponds to values of the fractional radius above 0.95. Another region of special interest is the vicinity of the bottom of the convection zone at  $r \approx 0.7 R_\odot$  which corresponds to  $\lambda \approx 1.05$ , and is where the solar dynamo is believed to operate. We do not see any feature indicating either a  $P_4$  or a  $P_6$  distortion in this region. In the core region,  $\lambda \leq 0.3$ , there are not many points and no apparent trend. The same is observed in corresponding plots for the remaining sets. Finally, there is no apparent evidence of an interior  $P_2$  distortion beyond that due to centrifugal stretching.

A more fruitful way of probing the core may be to use the line-width data.

#### 4. Probing the Core with Line-Width Data

Probing the core is always problematic. Of course, we can do a better job with more precise frequencies and a richer spectrum. But perhaps a different approach could bring more immediate results. Goode and Thompson (1992) showed that an unsteady perturbation induces an effective line-width on a line that is otherwise perfectly sharp, and that this implies that line-width data can be used to place a limit on unsteady perturbations in the solar interior. For instance, Goode and Thompson (1992) assumed that the Sun's convection zone rotates on a single axis with surface-like differential rotation throughout, but that the radiative interior rotates as a solid body with its axis of rotation inclined to that of the convection zone. From the frame of a terrestrial observer, there is an unsteady perturbation resulting in an effective line width which depends on the inclination angle,  $\beta$ , of the core.

In Figure 7, we show how the  $m = 0$  component (where the symmetry axis is that of the rotating convection zone) of a single  $nlm$  mode is fractionated into mul-

multiple frequencies with  $m = 0$  by the unsteady perturbation. From the perspective of the observer, this introduces an effective line width, in the otherwise assumed to be sharp components, of about  $3 \mu\text{Hz}$  for  $\beta = 45^\circ$  and about  $1 \mu\text{Hz}$  for  $\beta = 10^\circ$ . Both of these line widths are far too broad to be consistent with the low-frequency line-width data. Using the line-width data represents a direct approach to determining the degree to which the Sun rotates on a single axis.

Another obvious unsteady perturbation is a deeply buried magnetic field. Goode and Thompson (1992) used BBSO line-width data to place a limit of about 30 MG on a buried field. The fields they selected were separately quadrupole poloidal and toroidal fields. The toroidal field approximates that given by Dicke (1982). Of course, such a field would also change the shape of the Sun's photosphere, and therefore could be detected in measurements of the solar shape. Since both shape and line widths are measured by MDI, it would be interesting to see what kinds of constraints can be placed by both kinds of data. They may have complementary aspects. In particular, if the buried field were aligned with the rotation axis, then it is likely that the line-width data would place the stronger constraint. However, the line-width data are less sensitive to an inclined field (Goode and Thompson, 1992), so that the distortion of the photosphere, which is relatively insensitive to the inclination, might place tighter constraints. However, the relative utility of the two approaches for constraining the core remains to be investigated.

### Acknowledgements

This work was supported in part by NASA-NAG5-4919 and NSF-ATM-97-14796.

### References

- Basu, S., Turck-Chièze, S., Berthomieu, G., Brun, A. S., Corbad, T., Gonczi, G., Christensen-Dalsgaard, J., Provost, J., Gabriel, A. H., and Boumier, P.: 2000, *Astrophys. J.* **535**, 1078.
- Bertello, L., Varadi, F., Ulrich, R. K., Henney, C. J., Kosovichev, A. G., Garcia, R. A., Turck-Chièze, S.: 2000, *Astrophys. J.* **537**, L143.
- Brown, T. M., Christensen-Dalsgaard, J., Dziembowski, W. A., Goode, P. R., Gough, D. O., and Morrow, C. A.: 1989, *Astrophys. J.* **343**, 526.
- Chaplin, W. J., Christensen-Dalsgaard, J., Elsworth, Y., Howe, R., Isaak, G. R., Larsen, R. M., New, R., Schou, J., Thompson, M. J., and Tomczyk, S.: 1999, *Monthly Notices Royal Astron. Soc.* **308**, 405.
- Dicke, R. H.: 1982: *Solar Phys.* **78**, 3.
- Duvall, T. L., Harvey, J. W., and Pomerantz, M. A.: 1986, *Nature* **321**, 500.
- Dziembowski, W. A. and Goode, P. R.: 1991, *Astrophys. J.* **376**, 782.
- Dziembowski, W. A. and Goode, P. R.: 1992, *Astrophys. J.* **394**, 670.
- Dziembowski, W. A. and Goode, P. R.: 1996, *Astron. Astrophys.* **317**, 919.
- Dziembowski, W. A., Goode, P. R., and Libbrecht, K. G.: 1989, *Astrophys. J.* **337**, L53.
- Dziembowski, W. A., Goode, P. R., Schou, J., and Tomczyk, S.: 1997, *Astron. Astrophys.* **323**, 231.

- Dziembowski, W. A., Goode, P. R., DiMauro, M. P., Kosovichev, A. G., and Schou, J.: 1998, *Astrophys. J.* **509**, L456.
- Goldreich, P. Murray, N., Willette, G., and Kumar, P.: 1991, *Astrophys. J.* **370**, 752.
- Goode, P. R. and Thompson, M. J.: 1992, *Astrophys. J.* **395**, 307.
- Goode, P. R., Dziembowski, W. A., DiMauro, M. P., Kosovichev, A. G., and Schou, J.: 1998a, in S. Korzennik and A. Wilson (eds.), *Structure and Dynamics of the Interior of the Sun and Sun-like Stars*, ESA, p. 887.
- Goode, P. R., Strous, L. H., Rimmele, T. R., and Stebbins, R. T.: 1998b, *Astrophys. J.* **495**, L27.
- Kuhn, J. R.: 1988, *Astrophys. J.* **331**, L131.
- Kuhn, J. R.: 1998, in S. Korzennik and A. Wilson (eds.), *Structure and Dynamics of the Interior of the Sun and Sun-like Stars*, ESA, p. 871.
- Libbrecht, K. G. and Woodard, M. F.: 1990, *Nature* **345**, 779.
- Ritzwoller, M. H. and Lavelly, E. M.: 1991, *Astrophys. J.* **369**, 557.
- Schou, J., Christensen-Dalsgaard, J., and Thompson, M. J.: 1994, *Astrophys. J.* **433**, 289.
- Schou, J., Kosovichev, A. G., Goode, P. R., and Dziembowski, W. A.: 1997, *Astrophys. J.* **489**, L197.